Silicon (2022) 14:2555–2563
https://doi.org/10.1007/s12633-021-01049-9

ORIGINAL PAPER

New Improved Thermoluminescence Magnesium Silicate Material for Clinical Dosimetry

Mohamed R. Abass[1] · Hassan M. Diab[2] · Mamdouh M. Abou-Mesalam[1]

Received: 15 January 2021 / Accepted: 3 March 2021 / Published online: 11 March 2021

Abstract

Magnesium silicate has been prepared by a precipitation technique. This composite structure was proven by different tools, XRD, TGA&DTA, FTIR, and XRF. Magnesium silicate was found to have the formulas $Mg_{1.1}SiO_{3.2}.1.1H_2O$. Thermoluminescence (TL) dosimetric properties like (linearity, fading, energy independence) of magnesium silicate in the shape of $MgSiO_3$ have been estimated. A strong TL dosimetry peak associated with gamma radiation arises from ^{137}Cs was developed. Different doses from gamma radiation were measured by thermoluminescence (TL) detection technique for magnesium silicate glasses in unique magnesium elements concentration to assess its dosimetric properties. A single strong peak of about 230 °C arises for all irradiated samples. Total integral values of TL output and TL of the principal peak values showing a linear behavior start with 0.5 Gray up to 2 Gray dose range. Correlation of magnesium silicate TL response and different doses showed dose-response improvement concerning low doses linear relationship.

Keywords Thermoluminescence · Magnesium silicate · Dosimetry; glow curve

1 Introduction

Inorganic substances of an ion-exchange type have recently played a great role, originally focused on their thermal and radiation resistance besides their chemical hazards [1–3]. Many years ago, a lot of studies about Thermoluminescence (TL) dosimetric properties have been achieved [4–11]. A process in which a luminescent substance exposed to radiation energy and being heated emits light is called the thermally excited light emission process. Absorbed ionizing radiation energy produced movable electrons inside the crystal lattice and some of them are trapped at lattice imperfections. Crystal heating releases some of these trapped electrons accompanied by light emission. The emission can be achieved using different excitation types of ionizing radiation such as gamma, X-ray, neutron, alpha, electrons, and beta radiation. The TL intensity is related to the trap

Highlights
- Magnesium silicate has been prepared by precipitation technique.
- Thermoluminescence (TL) dosimetric properties such as (linearity, fading, energy independence) of magnesium silicate in the form of $MgSiO_3$ have been estimated.
- A single strong peak of about 230 °C arises for all irradiated samples. Both integral TL output and TL of the principal peak values showed a linear behavior within the dose ranges from 0.5 up to 2 Gy.
- The correlation of magnesium silicate TL response and different doses demonstrated dose-response improvement regarding the low doses linear relationship.

✉ Mohamed R. Abass
mohamed.ragab2014300@yahoo.com;
mohamed.ragab@eaea.org.eg

Hassan M. Diab
hdiab2003200327@yahoo.com

Mamdouh M. Abou-Mesalam
mabumesalam@yahoo.com

[1] Hot Laboratories Center, Egyptian Atomic Energy Authority, Cairo, Egypt

[2] Radiation Dosimetry Laboratory, National Institute of Standards, Giza, Egypt

activation energy level through certain expressions when the heating rate is linear under the condition of the probability of second trapping to be negligible for the probability of recombination, so that determines the trap depth could be possible.TL glow peaks in Thermoluminescence (TL) studies related to the structures of the defects giving rise to these peaks [4, 5]. Under various conditions of dose, annealing and storage parameters, LET of the radiation field, etc. Each glow peak may have distinctly different dosimetric characteristics and the relative intensity of the various glow peaks depends on a great many factors. However, the dosimetric characteristics of the glow peaks rather than the glow curve (integration over several glow peaks) will surely lead to a better understanding of TLD and contribute to the adoption of a better dosimetric technique. So, there is a need to synthesis a new TL material that has a simple glow curve and glows peak. LiF is considered the most famous material used in thermoluminescence detection techniques it is used in different applications, such as; environmental, personal, besides clinical dosimetry. Many different chips are available according to various dopant concentrations [8]. Uses of thermoluminescence (TL) phenomenon for suitability testing of glasses being an interesting subject in recent years through radiation-induced defect centers investigations for more technical applications in photonics [12–17]. Thermoluminescence behaviors of $Sr_3MgSi_2O_8$ phosphor doped with Dy^{3+} were studied by [18]. Also, Chen's method has been utilized for determining the kinetic measurable factors for glow curve deconvolution. Recently, investigation of borosilicate glass glow curves which has a composition $(60-x)B_2O_3-20SiO_2-10Na_2O-10MgO-xDy_2O_3$ doped with rare earth after different dose irradiated with high doses of gamma radiation achieved. Samples doped with 0.6% mol Dy^{3+} showed appropriateness for dosimetric utilizations because of their good thermoluminescence dose sensitivity and response [19]. Furthermore, TL glow curves for 2 mg $Sr_3MgSi_2O_8$ substance exposed to irradiation by 254 nm UV source showed a resolute single peak around 123 °C. A glow curve deconvolution technique was used for analyzed acquired glow curves [20]. Moreover, magnesium orthosilicate intensity of TL glows curves showed a good dose-response linear relationship extended to 20 Gy. To a certain degree, TL features of this phosphor are conditional beside Mg_2SiO_4 is suggested to consider as a suitable substance for dosimetry [21]. Also, the photon shielding properties of a glassy system composed of $20Li_2O–(70\text{-}x)B_2O_3–10MgO–xTm_2O_3$ doped with different Tm_2O_3 oxides (where $0 \le x \le 1$) were investigated utilizing the advanced program (XCOM). When the Tm_2O_3 concentration rise, the mass attenuation coefficients also increased. The variation of Tm_2O_3 concentration affecting the good properties of LMB glasses. It appeared that the glass compositions recommended for solid-state lasers usage [22]. For new sets telluroborate glasses doped of Sm^{3+} with varying TeO_2 content, gamma shielding properties were testing utilizing MCNPX code from energy range from 0.356up to 1.33 MeV. when the TeO_2 content changes from 0 up to 40% mol for all glasses, the calculated mass attenuation coefficient showed an increasing behavior principally at an energy value 0.356 MeV, 4TBS glass material displayed the lowest value of half-value layer. The study assures that the alteration of B_2O_3 by TeO_2 supports the capability of the prepared glassy materials to minimize the gamma photons [23]. Furthermore, TL dosimetric properties for rare-earth-doped tellurite form glasses were examined [13]. Thermoluminescence kinetic parameters examination were used also for glasses of Binary lead silicate type [14], In recent work, prepared magnesium silicate glasses glow curves were testing for dosimetry considering glass structure correlating with different dosimetric properties.

2 Experimental Work

Magnesium silicate was fabricated as reported [24–26], by additional dropwise of Na_2SiO_3 to $MgCl_2{\cdot}6H_2O$ equimolar solutions (0.5 M), which have a volumetric ratio of Mg/Si = 1.5 at constant agitation at 25 ± 1 °C. When the addition was finished, that diluted NH_3 was added until a precipitate was formed, and instead, the reaction mixture was kept undisturbed overnight. With 0.1 M HNO_3, a precipitate was washed to remove Cl^- and impurities. To kill NO_3^- a precipitate was cleaned with distilled H_2O. It was soaked several times with H_2O distilled [24, 27]. Magnesium silicate was dried and ground in a powder form and mixed to a ratio of 1:5 with KBr, then pressed to the IR analysis. FTIR was performed on a computerized spectrophotometer ranges from 4000 up to 400 cm^{-1}, KBr discussing the Genesis-IIFT-IR spectrometer. The Philips series x-ray spectrometer-2400 was used to evaluate the stoichiometry of the components in magnesium silicate. The prepared composite was analyzed by XRD using Shimadzu XD-D1. Measurements were done with a speed of 2 °/ min in 2θ ranges from 4 to 90. Composite fabricated (20 mg) were analyzed for DTA &TGA with a Shimadzu DTG-60H. Harshaw 4500 TLD reader within a planchet heating pathway used for measuring thermoluminescence response. The glass being closed to a stainless-steel crucible for the heating process; a thermocouple closely connected to the sample holder. After irradiation, heating of the sample achieved by a steady rate equal to 1.5 °Cs^{-1} extends from 50 °C up to 400 °C. This method assures set sample doses to zero and subsequently no need for more annealing steps. TL dose-response within dose range starts from 50 °C up to 400 °C sample doses expressed by an integral value. ^{137}Cs standards source located at the laboratory of ionizing radiation metrology. National Institute of standards was used, its half-life of 30.17 years. The utilized source was manufactured in Canada with a 23 rad/min at a distance of 30 cm on work time. The 2570 farmer-type dosimeter, made in the U.K. by accompany of Nuclear Enterprises Ltd. attached to an ionization chamber with serial number 2571 which is sensitive to gamma rays under the ideal condition of temperature and pressure to observe the dose

Scheme 1 Magnesium silicate forming mechanism

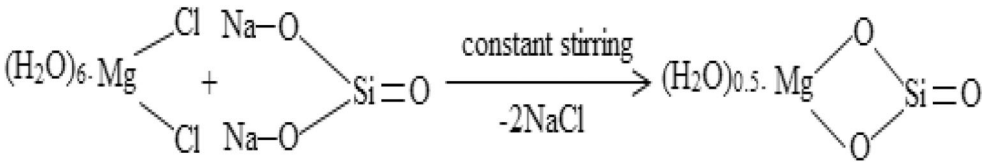

rate of ^{137}Cs source. The dosimetric properties were achieved with gamma photons from ^{137}Cs source. The dose was computed by the IAEA code of practice with a 2.5% accuracy value. Every TL- measurement carried out was repeated three times with a net standard deviation equal to ±2%. The average reproducibility for glasses is 0.82% which means (1 standard deviation), evaluated by 4500 planchet heating reader, manual type. If the dosimetry process based on accuracy and good repeatability reading values are required, it must be careful about the distribution of glasses powder on sample holders at the manual planchet reading mode. All samples measurements achieved with uniform patch homogeneity.

3 Results and Discussion

As already stated in the experimental section, magnesium silicate was fabricated and has a hard granulating in nature with white color. Magnesium silicate formation mechanism (Scheme 1), was obtained by replacement of $2Na^+$ by Mg^{2+} and 2 NaCl molecules were withdrawn.

Magnesium silicate IR spectrum (Fig. 1 & Table 1). This Figure displays six characteristic bands. The first vibration of H_2O and OH absorbed in the composite appeared at 3150–3670 cm^{-1} [1]. Owing to a bending vibration for H_2O in magnesium silicate, a high absorption band showed at 1652 cm^{-1} [1, 31–33]. Mg-O resulted in a band of 1000 to 1100 cm^{-1} [1, 28]. Mg-OH deformation vibration resulted in a band at 903 cm^{-1} [29]. Mg-O-Si & Si-O-Si bending vibrations are connected to two 640 & 470 cm-1, respectively [30].

XRD for magnesium silicate (Fig. 2), reveals that a prepared composite has a crystalline structure. These results were consistent with XRD data from composites operated at different heating temperatures [1, 34].

TGA & DTA chart for magnesium silicate heated at a rate of 10 °C/min (Fig. 3), through a three-step procedure. A first-stage (43–192 °C) may be due to free water loss [1, 35], a weight drop in this heating area is (8.2%). A second-stage (192–283 °C) resulted from a break down for residual OH & unbonded oxygen condensation [36], a weight drop in this heating area is (4.45%). A third-stage (283–800 °C) may be attributed to chemical bond water lost [1], a weight drop in this heating area is (12.8%). DTA shows that 2 endothermic peaks about (128 & 501 °C) could be attributed to free water & chemical bond water loss, respectively. A single exothermic peak arises at (257 °C) explained by a release of residual OH decay & unbonded oxygen condensation. From TGA data (Fig. 3), a weight loss for composite prepared is extended to 700 °C, and no weight drop happened within a range from 700 up to −800 °C. This enhancing the fact that composite prepared has much more thermal stability than other materials. The weight drop for magnesium silicate with the heating temperature that a (33.4%) weight drop obtained if a substance exposed to calcination process about 800 °C.

A chemical structure for prepared composite depends on the information get from XRF and TGA& DTA thermograms about elemental analysis whose mass drop allows calculating an amount of H_2O found in a matrix by an equation:

$$18n = \frac{X(M + 18n)}{100} \quad (1)$$

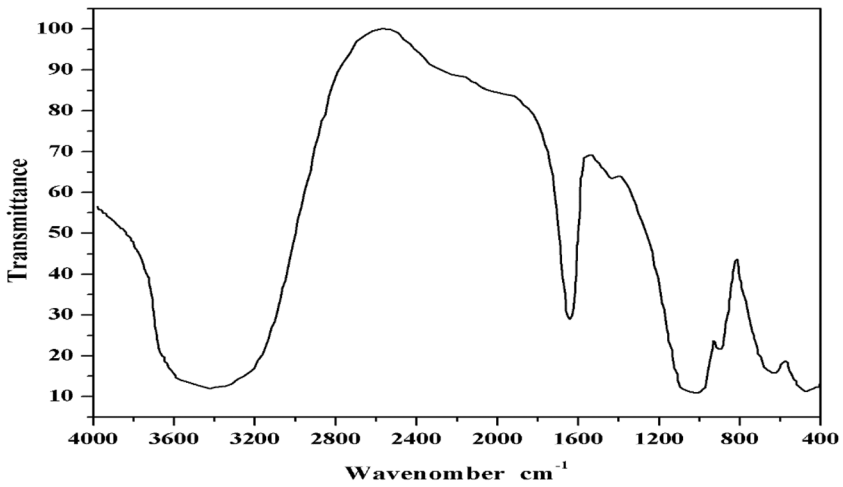

Fig. 1 IR spectrum for magnesium silicate

Table 1 Assignments of IR bands (cm^{-1}) for magnesium silicate

Wavenumber (cm^{-1})	Intensity	Assignments	References
3150–3670	b	. OH and . H_2O	[1]
1652	s	δ. H_2O	[1]
1000–1100	b	δ. (Mg-O)	[1, 28]
903	s	δ. Mg-OH	[1, 29]
640	b	δ. Si–O–Mg	[1, 30]
470	b	δ. Si–O–Si	[1, 30]

Where b is broad and s is strong

In which X is a mass drop percent of H_2O, n represents H_2O mole number, & M represents a compound molar mass without water molecules [1]. In which X is a mass drop percent of H_2O, n represents H_2O mole number, & M represents a compound molar mass without water molecules [1]. An X value for magnesium silicate was 8.2%. The molecular formula of magnesium silicate was calculated and indicated that $Mg_{1.1}SiO_{3\cdot2}.1.1H_2O$.

The relationship between impacts of different grain sizes on TL sensitivity (Fig. 4) reveals that TL intensity reduced when the grain size enlarged so that reduction of collection efficiency of measured radiation, and the other way round. The grain size range of magnesium silicate is located between 53 and 106 with SD = 0.005.

The glow curve model of magnesium silicate samples is shown in Fig. 5 with 1.5 °C/s heating rate at different irradiated low doses (0.5 Gy - 2 Gy). A strong main peak located around 230 °C. As the dose increased the peak location doesn't change, but the thermoluminescence response increases linearly. For a maximum point of peak height, a linear relationship with dose is noticed, which suppose uses this point for dose monitoring. This peak is considered prevalent for doses extended from 0.5 Gy - 2 Gy. It is a stable peak. Dosimeter material including magnesium has a good sensitivity resulted from the large cross-section of magnesium element suggesting many large areas of traps. A reason for the peak broadness could be explained by the closeness of spaced trapping centers responsible for individual peaks which suggest its hard resolving process. This suggests a glass doped with magnesium impurities is an ideal complex trapping system. It is recommended to express the results to detect and monitor the dose as peak heights because of minimal dissipation than peak areas and better spatial resolution, for the center glow peak located at 230 °C, trap parameters such as kinetics order (b), activation energy (E), and also frequency factor (s) were calculated. Dosimetric 230 °C glow peak for gamma-irradiated samples extended from 0.5 Gy - 2 Gy doses utilizing the Chen method which is dependent on glow curves shape [37].

The use of thermal peak temperature to obtain activation energy (E) from the next equation [38, 39]:

$$E = C_\gamma\left(\frac{KT_m^2}{\gamma}\right) - b_\gamma(2KT_m) \tag{2}$$

Kinetics order (b) may be detected by computing a glow peak symmetry factor (μ_g). From shape parameters of well-known values [37, 38] according to:

$$\mu_g = \frac{\delta}{\omega} = \left(\frac{T_2 - T_m}{T_2 - T_1}\right) \tag{3}$$

δ is selected as ($\delta = T_2 - T_m$) cδ & bδ have a values of 1.71 & 0, respectively. Where T_1 & T_2 are temperatures of half-intensity centering low & high-temperature peak borders, respectively. μ_g for 230 °C thermal peak for Mgsi determined to be 0.51, which indicates that this peak follows a second-order

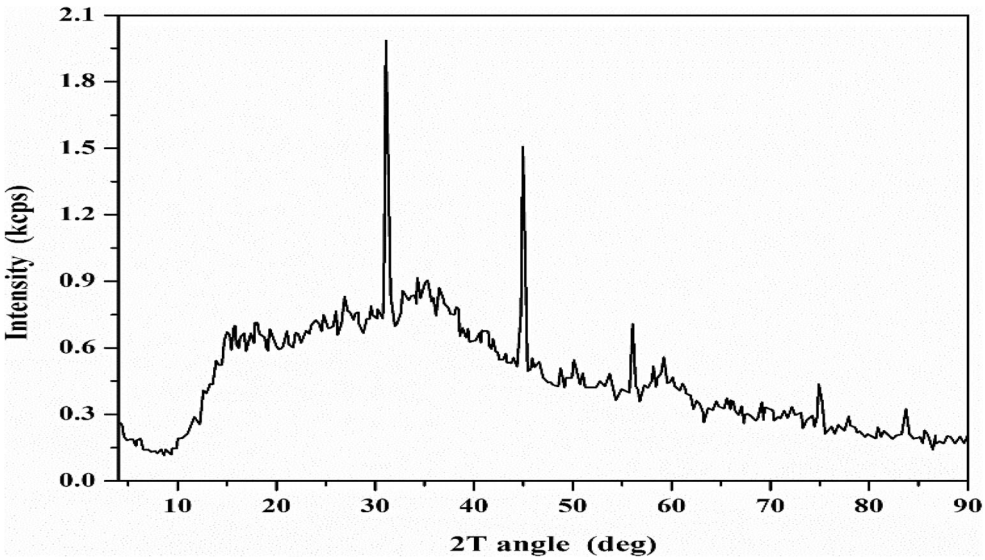

Fig. 2 XRD for magnesium silicate

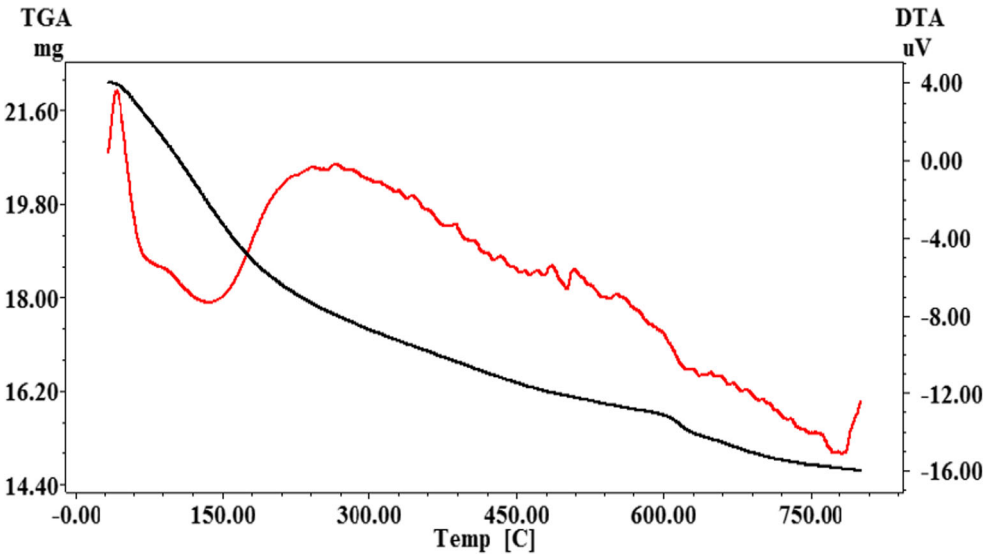

Fig. 3 DTA&TGA for magnesium silicate

reaction kinetics. When activation energy E and kinetics order were determined, a frequency factor S can be estimated by the next equation [38, 39]:

$$\frac{\beta_E}{KT_m^2} = S\left(1 + (b{-}1)\frac{2KT_m}{E}\right)\exp\left(-\frac{E}{KT_m}\right) \quad (4)$$

Assuming ß is a heating rate, the calculation of frequency factor S is $1.11\times 10^7\ s^{-1}$ concerning the former traps filling next to the excitation and therefore on the dose responsible for excitation [40, 41].

A process of sample preparation was the precipitation reaction at 25 ± 1 °C. An arrangement of traps created using the γ-radiation process may be changed by the alteration for concentrations of substances i.e. concerning a radiation impacts in inorganic dosimetry, enhancement of concentrations leads to thermal activation energy (E) increased. For all TL output, the studied concentration range was favorable.

In both Fig. 6 and Fig. 7, for glass doped within magnesium, different doses and subsequent TL-response represented an integral peak value and peak height. For low doses, magnesium ions doped host material showed a TL-response in a linear relationship. The straight line has a slope = 1 from a glow peak temperature trap depth E could be determined by eq. (5):

$$E = C\left(\frac{KT_m}{2}\right) - b(2KT_m) \quad (5)$$

Where T_m: temperature of a thermal peak, K: Boltzmann constant T_m picked up as a high-temperature half-width ($T_2 - T_1$), C & b values are considered as constants of peak shape. In the case of the second-order equation, C value: 2.54 and b value: 1. the trap depth [E] of the sample's principal peak that arises at 230 °C was determined as 1.18 eV. Densities of trapped carriers are represented by peak intensity and trap depth affecting recombination among holes and excited electrons. As seen in Figs. 6 and 7. The relative TL intensity for MgSi samples expressed in terms of different gamma doses, TL dose-response curve was observed in linear behavior inside dose range start with 0.5 Gray - 2 Gray. Suggesting that the suitability for radiotherapy applications. The

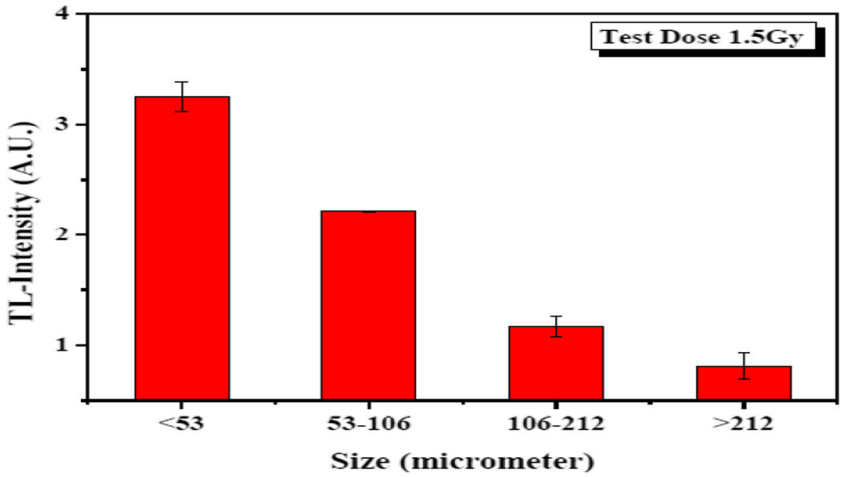

Fig. 4 The grain size effect on the TL-sensitivity. The error in the size range 53–106 is SD = 0.0049

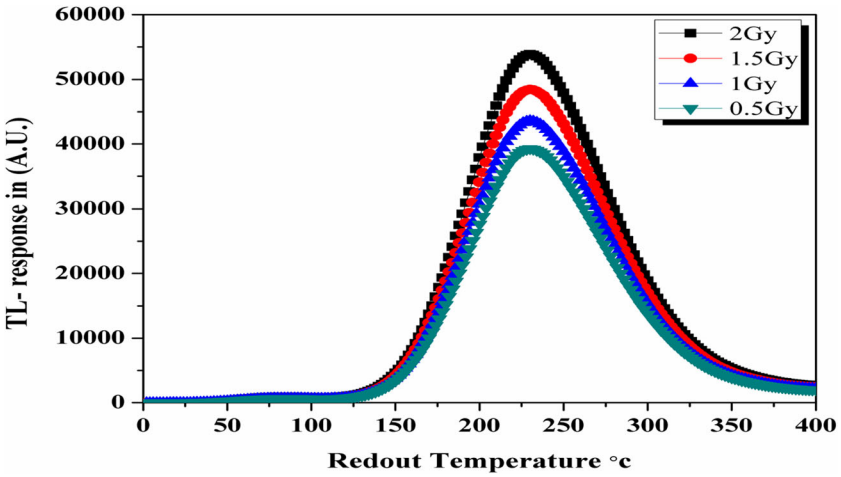

Fig. 5 The different glow curves for different doses for magnesium silicate

straight-line slope value is 1.25. From a dosimetric point of view, glow curves integral value under 230 °C peaks is utilized to absorbed dose calculation The linear part expressed by eq. Y = 1.25 x + b where Y: represent TL-response in arbitrary units and X considered absorbed dose represented in the gray unit. The extrapolation to Y-axis and equal: 360, a: represent slope amount = 1.25. The TL–dosimeter response can be calculated from this relationship and the absorbed dose can be also deter-

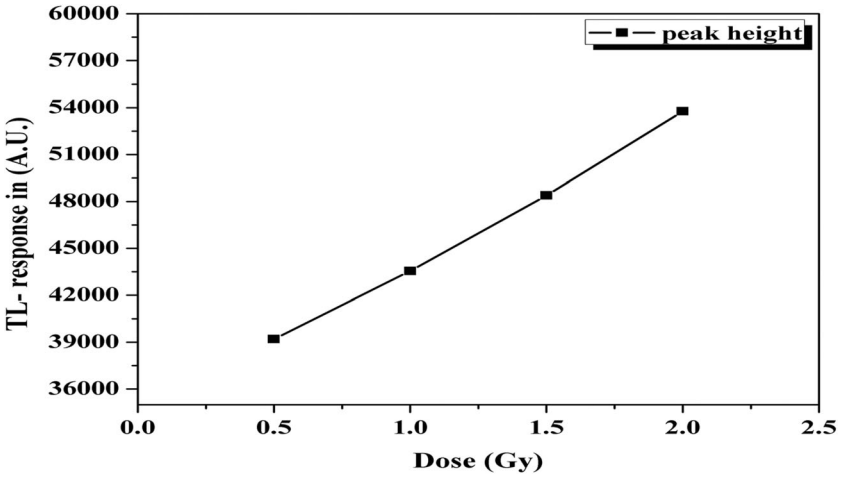

Fig. 6 TL response vs. dose of magnesium silicate irradiated with ^{137}Cs photons. TL response is represented by peak height from 0 °C up to 360 °C

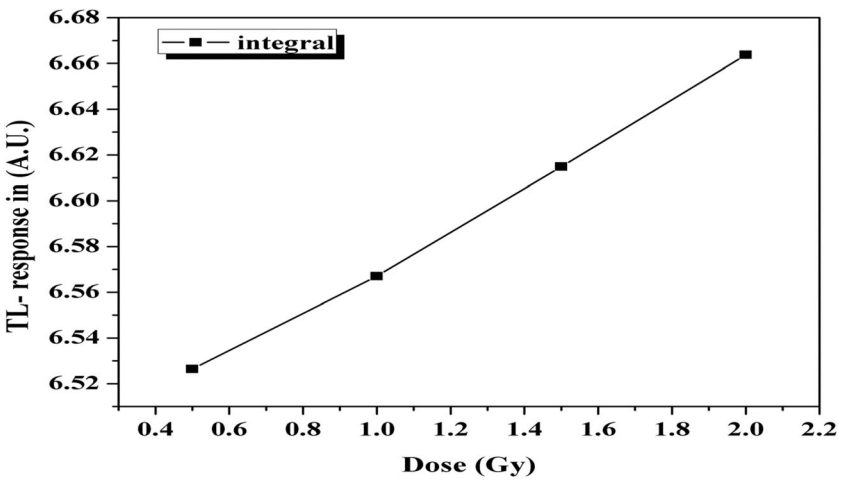

Fig. 7 Dose against TL response of magnesium silicate irradiated with ^{137}Cs photons. TL response is represented by an integral value from 0 °C up to 360 °C

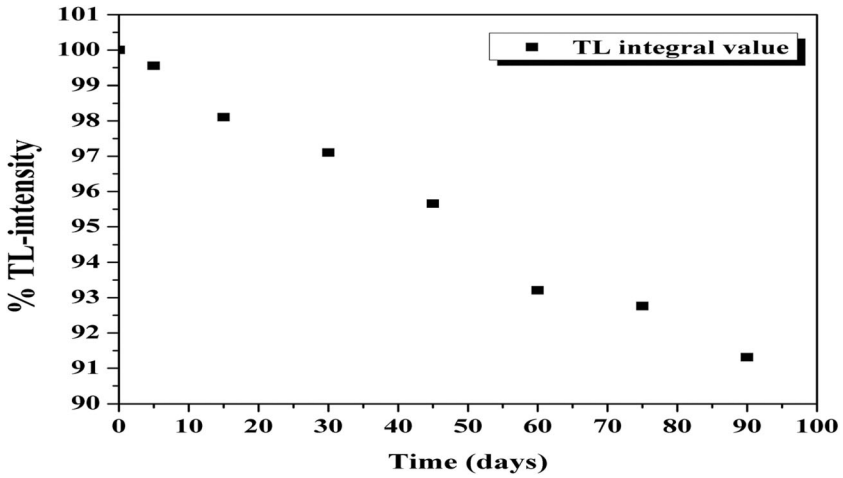

Fig. 8 The fading process is represented by the TL-intensity of different dosimeters at room temperature

mined. The sensitization process is due to competition mechanisms between the deep hole and electron traps in both stages of the irradiation and heating of the TL process. Considering that the difference filling effect of these traps. It should be paid attention that the central dosimetric trap is an electron trap, while deep electron traps full of lead to minimizing competition, which leads to sensitization. While deep hole traps filling of could increases competition, causing desensitization. As a result of the existence of these competitors, the recombination real number (i.e., the TL signal) post-dose irradiation will depend primarily on the deep trap occupancy. Therefore, sensitivity changes according to filling or emptying these deep levels are expected to cause.

Determination of fading is the main trouble in the thermoluminescence (TL) tool found in dosimetric scope, looks like personnel, clinical dosimetry, and environmental dosimetry [42]. When the accumulated TL signal or trapped charges after irradiation exposed to leakage, this operation is called the thermal fading effect. Figure 8, shows the integral value of TL-intensity after stored silicate material used for 90 days. The fading or leakage percent value equal to 9% regarding the composition of magnesium silicate itself. To verify the stabilization state process, the TL measurements were carried out after 30 min for each. This similar time interval after irradiation removes the signal of a lower temperature peak.

Not only trapping centers ionization can explain the fading process of MgSi but also it should be considered as the second operation in silicates which is the diffusion of oxygen. Concerning silicate materials energy dependence, prepare 5 groups as energy points. At every point at least has 6 TLDs, every group irradiate with a dose of 2Gy at a particular fixed energy. TL-intensity as an integration value after irradiation of glassy materials with 2 Gy at different radiation energies (Fig. 9), different energies of the silicate samples showed a fixed dose-response relationship at a certain dose which recommend remarkable behavior of energy-independent for these materials.

Table 2, shows dosimetric characteristics of thermoluminescence technique including a domain of doses, method of annealing, spectrum shape, dose information, readout technique, the sensitivity of the sample, physical forms for magnesium ions glass doped, trap depth activation energy found to be 1.18 eV because of more heat is needed to estimate the particular peak around 230 °C which is responsible for dosimetry. Thermoluminescence response of therapeutic dose ranges from 0.5 Gy - 2 Gray against the transferred dose

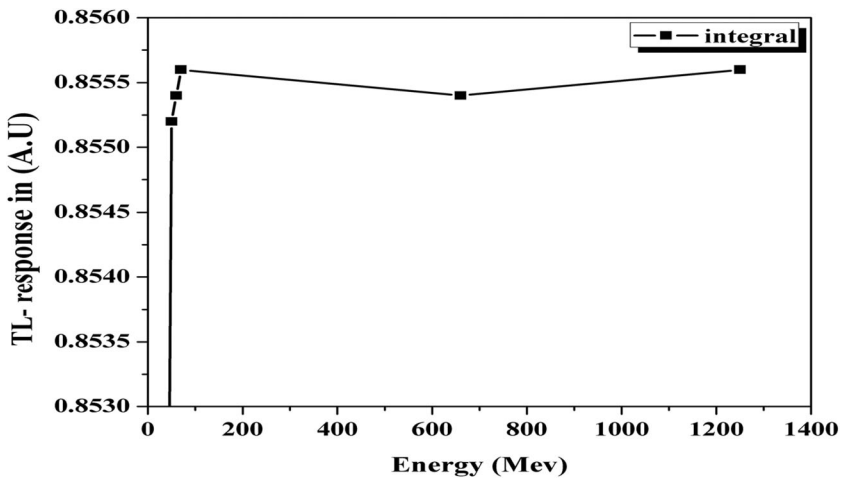

Fig. 9 The energy-dependent process is represented by the TL-intensity of different dosimeters at room temperature

Table 2 TL properties summary of magnesium silicate

Dosimetric properties	
Dose Range: Gray (Gy)	From one-half Gy extend to `two Gy
Dose-Response: Coulomb (C)	Linear From one-half Gy to two Gy
Annealing method: The degree Celsius (°C)	150 min at 400 °C
Application	Clinical Dosimetry
Spectrum peak at The degree Celsius (°C)	230 °C
Response Readout techniques	Destructive
Dose information	Temporary
Physical shape	Pellets and powder shapes
Activation energy: electron volt (eV)	1.18

without approach saturation level gives a chance in the future to utilize these modified samples in a phantom for review dose distribution treatment planning. The experimental data revealed that the magnesium silicate affected quantitatively but not qualitatively by the radiation TL- response according to the irradiated doses variance resulted from different created trap centers.

4 Conclusion

From previous results it may be deducted that;

- ❖ Magnesium silicate was prepared by precipitation technique. The patterns of XRD show that magnesium silicate has a crystalline structure.
- ❖ Concerning doping oxides type similar created trap centers resulted in. So that the sensitivity and response of TL-radiation based on the magnesium silicate constitution quantitatively only.
- ❖ TL dose-response from 0.5 Gray - 2 Gray in radiotherapy range application against the transmitted dose which is not reached saturation level gives a probability to utilize this glassy samples for the count the dose received by a phantom tumor patient.
- ❖ Good gamma radiation TL response makes the magnesium ions doped silicate an improvement material for gamma dosimetry. This property has an important purpose in manufacture selective dosimeters appropriate for investigating the biological influence due to exposure to gamma radiation.
- ❖ The data obtained from this paper offered good thermoluminescence dosimetric benefits of the inspected magnesium silicate which recommended the potential use of this material as gamma-ray thermoluminescence detectors.

Acknowledgments This word has been supported by the Egyptian Atomic Energy Authority and National Institute for Standards, Egypt. Great thanks to all members of the nuclear fuel technology department, Egyptian Atomic Energy Authority for supporting this work.

Availability of Data and Material Yes

Author Contribution **M.R. Abass**: Data curation, writing - original draft review & editing. **H.M. Diab**: experimental work & editing. **M.M. Abou-Mesalam**: experimental work.

Declarations Yes

Consent to Participate Yes

Consent for Publication Yes

Conflict of Interest The authors whose names are listed immediately below certify that they have NO affiliations with or involvement in any organization or entity with any financial interest (such as honoraria; educational grants; participation in speakers' bureaus; membership, employment, consultancies, stock ownership, or other equity interest; and expert testimony or patent-licensing arrangements), or non-financial interest (such as personal or professional relationships, affiliations, knowledge or beliefs) in the subject matter or materials discussed in this manuscript.

Mohamed R. Abass, Hassan M. Diab, and Mamdouh M. Abou-Mesalam.

References

1. Abou-Mesalam MM, Abass MR, Abdel-Wahab MAet al (2016) Complex doping of d-block elements cobalt, nickel, and cadmium in magneso-silicate composite and its use in the treatment of aqueous waste. Desalin Water Treat 57:25757–25764. https://doi.org/10.1080/19443994.2016.1156031
2. Ismail L, Khalili F, Orabi FMA (2020) Modification of Silica Nanoparticles with Cysteine or Methionine Amino Acids for the Removal of Uranium (VI) from Aqueous Solution. Silicon 12: 2647–2661
3. Wakabayashi S, Takahashi S, Matsunami H, Hamamatsu S, Hachinohe M, Kihou N, Yamaguchi N (2020) Evaluation of ^{137}Cs ageing by dynamics of ^{137}Cs/^{133}Cs ratio in andosol paddy fields with/without potassium fertilizer application. J Environ Radioact 218:106252
4. El-Mallawany R, Diab HM (2012) Improving dosimetric properties of tellurite glasses. Phys B Condens Matter 407:3580–3585
5. Diab HM (2005) Luminescence properties of Sm^{3+} in strontium tetraborate for assessment of electron beam dosimetry. Radiation Effects & Defects in Solids 160:137–143
6. El-Mallawany R, Diab HM (2013) Effect of pre-readout annealing treatments on TL mechanism in tellurite glasses at therapeutic radiation doses level. Measurement 46:1722–1725
7. Abdel Ghaffar AM, El-Arnaouty MB, Diab HM, Hegazy E-SA (2009) Radiation synthesis of grafted polymers for studying thermoluminescence characterization and its possible application as a dosimeter at low doses. Polym-Plast Technol Eng 48:423–431
8. Diab HM, Abdelghany AM, Hafez HS (2020) Dosimetric behavior of modified borate bioglass containing copper for low photon dose measurements using luminescence characteristics. Journal of Materials Science: Materials in Electronics 31:20452–20459

9. Diab HM, El-Mallawany R (2014) Estimation of uncertainty for sulfonated grafted low-density polyethylene dosimeter using thermoluminescent dosimeter. Measurement 47:22–25
10. Diab HM, Ghaffar AMA, El-Arnaouty MB (2005) Thermoluminescence characterization of functionalized grafted polymers and its application for radiation dosimetry at low doses. Radiation Effects & Defects in Solids 160:401–416
11. Abd-Elghany AA, Diab HM, Sulieman A (2020) Determination of electron radiation dose uncertainty for strontium tetraborate doped with samarium. Journal of Radiation Research and Applied Sciences 13:246–251
12. Dubey N, Dubey V, Saji J, Kaur J (2020) Thermoluminescence glow curve analysis and trap parameters calculation of UV-induced $La_2Zr_2O_7$ phosphor doped with gadolinium. J Mater Sci Mater Electron 31:1936–1944
13. Chialanza MR, Castiglioni J, Fornaro L (2012) Crystallization as a way for inducing thermoluminescence in a lead borate glass. J Mater Sci 47:2339–2344
14. Rayan DA, Elseman AM, Rashad MM (2018) Remarkable impact of Ni^{2+} ion on the structural, optical, and magnetic properties of hexagonal wurtzite ZnS nanopowders. Applied Physics A 124:1–10
15. Marrale M, Longo A, Bartolotta A, D'Oca MC, Brai M (2013) Preliminary application of thermoluminescence and single aliquot regeneration method for dose reconstruction in soda lime glass. Nucl Instrum Methods Phys Res, Sect B 297:58–63
16. Khan A, Khuda F, Elseman AM, Aly Z, Rashad MM, Wang X (2018) Innovations in graphene-based nanomaterials in the preconcentration of pharmaceuticals waste. Environmental Technology Reviews 7:73–94
17. Khan A, Xing J, Elseman AM, Gu P, Gul K, Ai Y, Jehan R, Alsaedi A, Hayat T, Wang X (2018) A novel magnetite nanorod-decorated Si-Schiff base complex for efficient immobilization of U (VI) and Pb (II) from water solutions. Dalton Trans 47:11327–11336
18. Dewangan P, Bisen DP, Brahme N, Tamrakar RK, Upadhyay K, Sharma S, Sahu IP (2018) Studies on thermoluminescence properties of alkaline earth silicate phosphors. J Alloys Compd 735:1383–1388
19. Kaur R, Bhatia V, Kumar D, Rao SMD, Pal Singh S, Kumar A (2019) Physical, structural, optical, and thermoluminescence behavior of Dy2O3 doped sodium magnesium borosilicate glasses. Results in Physics 12:827–839
20. Dewangan P, Bisen DP, Brahme N et al (2019) Thermoluminescence glow curve for UV induced $Sr_3MgSi_2O_8$ phosphor with its structural characterization. J Mater Sci Mater Electron 30:771–777
21. Dogan T, Akça S, Yüksel M, Kucuk N, Ayvacikli M, Karabulut Y, Canimoglu A, Topaksu M, Can N (2019) Comparative studies on thermoluminescence characteristics of non-doped Mg_2SiO_4 prepared via a solid-state reaction technique and wet-chemical method: an unusual heating rate dependence. J Alloys Compd 795:261–268
22. Mhareb MHA, Almessiere MA, Sayyed MI, Alajerami YSM (2019) Physical, structural, optical and photons attenuation attributes of lithium-magnesium-borate glasses: role of Tm_2O_3 doping. Optik 182:821–831
23. Divina R, Marimuthu K, Sayyed MI, Tekin HO, Agar O (2019) Physical, structural, and radiation shielding properties of B_2O_3–MgO–K_2O–Sm_2O_3 glass network modified with TeO_2. Radiat Phys Chem 160:75–82
24. Abou-Mesalam MM, Abass MR, Ibrahim AB, Elseman AM, Hassan AM (2019) Tunable optical and dielectric properties of polymeric composite materials based on magneso-silicate. Bull Mater Sci 42:31
25. Abou-Mesalam MM, Abass MR, Ibrahim AB, Zakaria ES (2020) Polymeric composite materials based on silicate. III-capacity and sorption behavior of some hazardous metals on irradiated doped polyacrylamide acrylonitrile. Desalin Water Treat 193:402–413. https://doi.org/10.5004/dwt.2020.25816
26. Abou-Mesalam MM, Abass MR, Abdel-Wahab MA, Zakaria ES, Hassan AM (2018) Polymeric composite materials based on silicate: II. Sorption and distribution studies of some hazardous metals on irradiated doped polyacrylamide acrylic acid. Desalin Water Treat 109:176–187. https://doi.org/10.5004/dwt.2018.22084
27. Abass MR, El-Masry EH, Ibrahim AB (2021) Preparation, characterization, and applications of polyacrylonitrile/ball clay nanocomposite synthesized by gamma radiation. Environ Geochem Health: 1–20. https://doi.org/10.1007/s10653-021-00813
28. Ali IM, Kotp YH, El-Naggar IM (2010) Thermal stability, structural modifications, and ion exchange properties of magnesium silicate. Desalination 259:228–234
29. Al-Degs YS, El-Barghouthi MI, Issa AA et al (2006) Sorption of Zn (II), Pb (II), and co (II) using natural sorbents: equilibrium and kinetic studies. Water Res 40:2645–2658
30. Madejová J (2003) FTIR techniques in clay mineral studies. Vib Spectrosc 31:1–10
31. Nassar AM, Zeid EFA, Elseman AM, Alotaibi NF (2018) A novel heterometallic compound for design and study of electrical properties of silver nanoparticles-decorated lead compounds. New J Chem 42:1387–1395
32. Rashad MM, Hassan AM, Nassar AM, Ibrahim NM, Mourtada A (2014) A new nano-structured Ni (II) Schiff base complex: synthesis, characterization, optical band gaps, and biological activity. Applied Physics A 117:877–890
33. Hassan AM, Nassar AM, Ibrahim NM, Elsaman AM, Rashad MM (2013) An easy synthesis of nanostructured magnetite-loaded functionalized carbon spheres and cobalt ferrite. J Coord Chem 66: 4387–4398
34. Abou-Mesalam MM, El-Naggar IM (2008) Selectivity modification by ion memory of magneso-silicate and magnesium aluminosilicate as inorganic sorbents. J Hazard Mater 154:168–174
35. Hamoud MA, Allan KF, Sanad WA, el-Hamouly SH, Ayoub RR (2014) Gamma irradiation-induced preparation of poly (acrylamide–itaconic acid)/zirconium hydrous oxide for removal of Cs-134 radionuclide and methylene blue. J Radioanal Nucl Chem 302:169–178
36. Abou-Mesalam MM (2003) Sorption kinetics of copper, zinc, cadmium, and nickel ions on synthesized silico-antimonate ion exchanger. Colloids Surf A Physicochem Eng Asp 225:85–94. https://doi.org/10.1016/S0927-7757(03)00191-2
37. Chen R (1969) On the calculation of activation energies and frequency factors from glow curves. J Appl Phys 40:570–585
38. Garlick GFJ, Gibson AF (1948) The electron trap mechanism of luminescence in sulphide and silicate phosphors. Proc Phys Soc 60: 574–590
39. Rasheedy MS (1993) On the general-order kinetics of the thermoluminescence glow peak. J Phys Condens Matter 5:633–636
40. Furetta C, Kitis G, Brambilla A, Jany C, Bergonzo P, Foulon F (1999) Thermoluminescence characteristics of a new production of chemical vapour deposition diamond. Radiat Prot Dosim 84: 201–205
41. Elkholy MM (2003) Thermoluminescence for rare-earths doped tellurite glasses. Mater Chem Phys 77:321–330
42. Pagonis V, Mian S, Mellinger R, Chapman K (2009) Thermoluminescence kinetic study of binary lead-silicate glasses. J Lumin 129:570–577